

Ronghui Zhou  
Ping Wang  
Hsueh-Chia Chang

Department of Chemical and  
Biomolecular Engineering,  
Center for Micro-fluidics and  
Medical Diagnostics,  
University of Notre Dame,  
Notre Dame, IN, USA

Received April 28, 2005  
Revised September 27, 2005  
Accepted October 2, 2005

## Research Article

# Bacteria capture, concentration and detection by AC dielectrophoresis and self-assembly of dispersed single-wall carbon nanotubes

The high polarizability and dielectrophoretic mobility of single-walled carbon nanotubes (SWNT) are utilized to capture and detect low numbers of bacteria and sub-micron particles in milliliter-sized samples. Concentrated SWNT solutions are mixed with the sample and a high-frequency ( $>100$  kHz) AC field is applied by a microelectrode array to enhance bulk absorption of the particles (bacteria and nanoparticle substitutes) by the SWNTs *via* dipole–dipole interaction. The same AC field then drives the SWNT–bacteria aggregates to the microelectrode array by positive-AC dielectrophoresis (DEP), with enhanced and reversed bacteria DEP mobility due to the attached SWNTs. Since the field frequency exceeds the inverse *RC* time of the electrode double layer, the AC field penetrates deeply into the bulk and across the electrode gap. Consequently, the SWNTs and absorbed bacteria assemble rapidly ( $<5$  min) into conducting linear aggregates between the electrodes. Measured AC impedance spectra by the same trapping electrodes and fields show a detection threshold of  $10^4$  bacteria/mL with this pathogen trapping and concentration technique.

**Keywords:** Biosensors / Dielectrophoresis / Nanotubes / Self-assembly

DOI 10.1002/elps.200500329

## 1 Introduction

Carbon nanotubes (CNT), representing one of the best examples of novel nanostructures, exhibit a range of extraordinary physical properties, such as extremely small size and high aspect ratio ( $>1000$ ), and a rich spectrum of electrical properties [1]. Exploiting these unique features to improve biosensors, bioelectronics, and circuitries have produced the rapidly developing fields of nanobioelectronics and nanobiotechnology [2]. Pioneering work from Dai's group [3, 4] has demonstrated that single-walled carbon nanotubes (SWNTs) could be used for small biomolecular and protein detection by measuring the detectable conductance change in

response to the physisorption of ammonia and nitrogen dioxide in physiological solutions. To improve reactivity and sensitivity, functionalizing CNT sidewalls with specific bio/chemical molecules ensure better chemical bonding between the nanotube and a specific chemical species as well as improve the selectivity of absorption process. Viruses binding to the surface of carbon nanotube devices through a suitable binding receptor immobilized on the devices result in a conductance change as well and may realize the long-term goal of single virus detection [5].

These biosensor applications that exploit the sensitive conductance change (or field-gating effects) of SWNT with respect to bioparticle docking, such as molecular, viral, cell, or organism, all employ pretemplated nanowires between two microelectrodes or on electrode surfaces. A large assembly of nanowire bridges across two long electrodes would have too high a conductance to allow detection of a small number of pathogens. As such, the target bioparticles should, ideally, be directed toward a small number of nanowires across two small and

**Correspondence:** Professor Hsueh-Chia Chang, Department of Chemical and Biomolecular Engineering, University of Notre Dame, Notre Dame, IN 46556, USA  
E-mail: chang.2@nd.edu  
Fax: +1-574-631-8366

**Abbreviations:** CFU, colony forming unit; DEP, dielectrophoresis; SWNT, single-walled carbon nanotubes

© 2006 WILEY-VCH Verlag GmbH & Co. KGaA, Weinheim



[www.electrophoresis-journal.com](http://www.electrophoresis-journal.com)

addressable electrodes. This transport to the micro- or nanosensors has become the rate-limiting step in light of the high sensitivity of nanotube sensors after the pathogen reaches the nanotube. Given a typical bioparticle diffusivity of  $10^{-7} \text{ cm}^2/\text{s}$ , it would require the bioparticle hours to diffuse across a realistic sample thickness of 0.1 cm to reach the sensor. This diffusion length can be reduced by dramatically increasing the bioparticle concentration. As a rough estimate, the effective diffusion length to the sensor is the average particle–particle separation. Consequently, for small bioparticles, especially submicron-sized bacteria or viruses, concentrations in excess of  $10^9$  particles per mL must be used to reduce the diffusion time to minutes. Such high concentrations are not realistic, especially for environmental samples, and a major technological bottleneck for biosensors, with or without nanotube amplification, is the reduction of transport time to the sensor.

One proposed technology for reducing the transport time of bioparticles is positive-AC dielectrophoresis (DEP) [6–9]. By using microelectrodes to sustain a nonuniform AC field with large penetration depth, the induced AC dipole of bioparticles with complex permittivity  $\epsilon^* = \epsilon + i\sigma/\omega$  results in a net force of

$$F_{\text{DEP}} = 2\pi a^3 \epsilon_m K \Delta E \quad (1)$$

where subscripts p and m denote particle and medium,  $E$  is the scalar intensity of the electric field in the medium, and  $a$  is particle size. The DEP direction is determined by the sign of the Clausius-Mossotti factor  $K$ ,  $\text{Re}((\epsilon_p^* - \epsilon_m^*)/(\epsilon_p^* + 2\epsilon_m^*))$ , where  $\text{Re}$  denotes real parts. This factor captures the interfacial polarization mechanism due to both internal and external dielectric dipole formation as well as the capacitive charging current of the double layer. The real medium permittivity  $\epsilon_m$  is used in Eq. (1) but that in the Clausius-Mossotti factor is complex with an imaginary component related to the medium conductivity  $\sigma_m$  and frequency  $\omega$ . Depending on the orientation of the AC dipole relative to the AC field, which depends in turn on the frequency of the field and the permittivity and conductivity of the particle and medium, the particle can move toward the high-field region (positive DEP) or low-field region (negative DEP). Positive DEP is the desired mobility if the objective is to move the particles toward an electrode sensor (with high field) embedded within the microelectrodes. However, for a typical bacteria and electrolyte medium, positive-DEP mobility for the bacteria only occurs at relative low frequencies below a critical crossover frequency of about several kHz [6, 8]. As will be shown subsequently, this frequency range is below the inverse  $RC$  time of most microelectrodes and the field penetration depth of the AC field is quite often only the Debye double layer thickness. This low frequency renders

the positive-DEP trapping field very short range and ineffective [6, 8] as a means of reducing the transport time between the bioparticles and the sensor.

Another strategy for transporting the bioparticles to the sensor is to produce focused AC EOF that can convect the particles rapidly [10, 11]. However, such AC EOF is only robust near the inverse  $RC$  time of the microelectrode array. Moreover, the bioparticles need to be trapped by DEP forces at the stagnation points of the AC EOF field. Since DEP is strongly size dependent, this trapping becomes weaker for submicron-sized bioparticles. The biosensors would need to be precisely placed at the stagnation points and the weak polarizability of the bioparticles renders the trapping difficult.

We demonstrate here a new submicron-sized bacteria trapping and detection strategy based on the various AC electrical and polarizability properties of SWNT's. Besides being good conductors, SWNT's are also known for their excellent rates of charge and discharge as super-capacitors, a property stemming from their high surface area in the double-layer charge storage mechanism [12]. However, application of this property to bioparticle sensing and biosensor technology is not extensively investigated. As for all good capacitor materials, SWNT's are endowed with a high electric permittivity and are easily polarizable in an electric field. For long SWNT's (length  $\sim 1 \mu$ ), such high polarizability produces strong dipoles. Attractive interaction between these strong induced dipoles explains the propensity of SWNT's to self-assemble into linear aggregates in an electric field [13, 14].

The high polarizability of SWNT should also endow them with large DEP mobility, another SWNT property that is not thoroughly investigated or exploited. Moreover, the conductivity of SWNT's is typically higher than the medium, thus rendering its DEP mobility positive even at frequencies higher than the inverse  $RC$  time of the microelectrode array. Consequently, the unscreened AC field of the electrodes is long-ranged and the SWNT's should migrate toward the electrodes with a high-positive-DEP mobility. They should also assemble into linear aggregates bridging two counter electrodes due to their high polarizability. This SWNT propensity to be trapped and to self-assemble into wires connecting two AC electrodes at high frequency, such that a conductance rise can be detected, would be extremely attractive for bacteria concentration and detection purposes. These application can be realized if the SWNT can be attached onto the bacteria, which would ordinarily exhibit weak-positive DEP at the high frequencies required for deep field penetration from microelectrodes. Bacteria are known to have high-ion capacitance [6], and an AC impedance measurement, instead of a DC conductance measurement, between the

same trapping electrodes can also produce more sensitivity for bacteria detection despite the large assembly of wire bridges.

Large numbers of SWNT's can be first dispersed in the sample such that the diffusion length between the bioparticle and the SWNT is determined not by the large average separation between bioparticle and the electrode sensor but by the much shorter (by a factor of 1000) separation between the bioparticle and SWNT. The latter separation is essentially the separation between the SWNT. The dispersed nanotubes not only reduce the diffusion distance but also increase the strength of local electrical field  $E$  and local electrical field gradient  $E$  around the nanotubes. Due to their specific composition and dimension, nanotubes inside the solution work as dispersed nanoscale electrodes. When an AC field is applied, the electrical field is strengthened at the dielectric discontinuities between the nanotubes and bulk solution. Such locally amplified fields and field gradients can promote the formation of induced dipoles on both SWNTs and the immersed bioparticles. Their DEP mobilities would hence be enhanced since the DEP force in (1) is due to a combination of the field, which is responsible for producing the particle dipole, and the field gradient to produce a net force on the resulting dipole. Such DEP mobility enhancement by the dispersed SWNTs would reduce the time for an encounter between a particle and an SWNT.

Moreover, the strong AC dipoles of the SWNT allow them to absorb onto the bioparticles, which also exhibit stronger AC-induced dipoles in the SWNT-enhanced fields, in the bulk solution. With sufficient SWNT absorption, the DEP mobility of the bioparticles can be enhanced by the absorbed SWNT with strong induced dipoles. Also, the particle-SWNT aggregate can now exhibit positive DEP at high frequencies exceeding the inverse  $RC$  time of the microelectrode array, as the positive DEP of the SWNT dominates the weak DEP of the particle at the aggregate. At these high frequencies, the field penetration depth of microelectrodes is comparable with the electrode dimension and yet the particles with absorbed SWNT are attracted to the high-field regions of the electrodes – an optimum scenario for an electrode bacteria sensor. Moreover, the bacteria-SWNT aggregate will participate in the wire assembly between two electrodes, allowing a detection mechanism for the trapped bacteria. This bioparticle capture and self-assembly *via* SWNT absorption will be demonstrated in this paper. The absorbed SWNT will be shown to produce positive-bacteria DEP at frequencies as high as 1 MHz, whereas the usual bacteria crossover frequency is less than 10 kHz. The absorbed SWNT will also be shown to significantly reduce

the transport time between the bioparticles and the sensor such that small numbers of submicron particles and bacteria (less than  $10^4$  particles per mL) can be concentrated and detected in less than 10 min. The same strategy should also work for viruses but our current facilities do not allow such verification.

## 2 Materials and methods

Gold electrodes designed for this study were patterned by lift-off: 5 nm Ti and 45 nm Au on a silicon dioxide microscope slides. Different styles of electrodes, parallel, perpendicular, and circle, were prepared and the gap width varied from 50 to 100  $\mu\text{m}$ . The electrode width is 50  $\mu\text{m}$ . A piece of CoverWell™ PC8R-0.5 (Grace Bio-Labs, OR) was place on top of electrodes to form fixed volume (50  $\mu\text{L}$ ) perfusion chambers. The vertical dimension of the chamber is about 500  $\mu\text{m}$ .

In a typical experiment, nanotube suspensions, with concentrations ranging from 0.05 to 0.2 mg/mL, were prepared by sonicating SWNT-COOH (Nanocs, NY, USA) in DI water for 30 min and left to sediment overnight before the upper homogeneous layer (approximately  $10^{12}$  SWNT per mL for a 0.1 mg/mL suspension) was used for further experiments (SWNT-COOH nanotubes is referred as SWNT for short). The nanotubes are estimated to be about 2–10 nm in diameter, 1  $\mu\text{m}$  in length, and an average weight of  $\sim 10^{-14}$  mg. Zeta potentials of the sonicated SWNT suspension was measured using a PALS Zeta Potential Analyzer Ver. 3.29 (Brookhaven Instrument, Holtsville, NY). Its noble metal electrode was preconditioned using DI water (10 runs, 30 cycles). The medium used for preconditioning was then removed from the holding cell, and an aliquot of the SWNT suspension was added to the holding cell and analyzed (10 runs, 20 cycles). The average zeta potential of SWNT was measured to be  $-40.80 \pm 1.47$  mV.

Fluoresbrite™ Polychromatic red microspheres (2.63% solids-latex, 500 nm or 1  $\mu\text{m}$  in diameter, Polysciences, PA), working as a substitute for submicron bioparticles, were diluted (1:10 000) in DI water (control sample) or in SWNT suspensions with identical concentrations. Prior to the experiments, *Escherichia coli* ( $\sim 1 \mu\text{m}$  with initial cell count of  $10^{10}$  colony forming unit (CFU)/mL) were washed in DI water three times and then resuspended in DI water or SWNT solution to acquire a cell count of  $10^{10}$ ,  $10^6$ ,  $10^5$ ,  $10^4$  CFU/mL, respectively.

Particle trapping rates were recorded for two concentrations of SWNT solutions (0.05 mg SWNT per mL and 0.1 mg SWNT per mL). The electric field across the electrodes was about 1 kV/cm, and the frequency was varied

from 100 to 5 MHz. Impedance and phase angle of the electrodes system were monitored by an Agilent 4284A impedance analyzer. The impedance equipment was connected to a computer recording system and a Lab-view software is used to collect all data. PBS, typically a mixture of 145 mM sodium chloride and 150 mM sodium phosphate with a pH of 7.2–7.4, was diluted 1:10, 1:100, and 1:1000, respectively, for comparison to SWNT solutions. DI water conductivity is roughly  $\sim 10^{-3}$  mS/cm (pH  $\sim$  6.0) while conductivity of PBS is around 0.015 mS/cm.

### 3 Results and discussion

Nanotube self-assembly was detected 0.5–5 min after applying an AC electric field under optical microscopy. SWNT exhibits positive DEP even at 1 MHz due to their high conductivity, as seen in Fig. 1. The linear aggregates that formed due to induced dipole–dipole (end-to-end) interaction are similar in dimension to SWNT self-assembly in organic solutions [15, 16], during chemical-vapor deposition with external field [17], or electric field-assisted growth and self-assembly of silicon nanowires [18]. However, the degree of branching of the linear aggregates and whether they bridge the two electrodes are sensitive to the field frequency. As seen in Fig. 1a, the SWNT self-assembly was confined to a thin boundary near the electrode and highly branched at low frequencies ( $<1$  kHz). Bridging did not occur even after 5 min. When the frequency was increased beyond 1 kHz to about 1 MHz in Fig. 1b, the SWNT self-assembled rapidly from both electrodes to form thin uniform wires that bridged the gap. The wires grew linearly from seeds on each electrode

until the other electrode was reached. After a number of wires had bridged the electrodes, there was a sharp decrease in the system AC impedance, which is a complex number corresponding to the AC voltage over the AC current. This reduction is shown as an increase in the slope of the AC conductance, defined as the inverse of the real part of the complex impedance in Fig. 2. It was evident from the figure that the conductance with bridged wires at 1 MHz was at least twice of that at 1 kHz. In Fig. 2 there was an increase in slope after 12 and 10 min at 10 and 100 kHz, respectively, indicating the contact between nanotubes that grew from two different electrodes. However, at 1 MHz, nanotube line-up started right after the activation of the electrical field and the slope was initially very high because of enhanced positive-DEP trapping of the SWNT at the electrode edges. The signal stabilized after about 1–3 min when the SWNT began to connect across the two electrodes. Since the self-assemble wires are visible under a microscope, we suspect they consist of bundles due to lateral aggregation of the SWNTs. Hence, the proposed particle absorption may be onto bundles instead of individual SWNTs. Nevertheless, we shall use SWNT as a general description for both.

There are two possible mechanisms for why the self-assembly is localized and branched at low frequencies. AC EOF [7, 10, 11] is present on the electrodes and such flows are known to be sensitive to the AC frequency. They can affect the self-assembly pattern by aligning the SWNT with viscous drag or by dragging the SWNT's away from the assembled patterns. However, the wires in Fig. 1c are oriented in the field direction and not the AC EOF direction as determined in our earlier work [11, 19]. Also, there is little flow in the electrode gap that is along

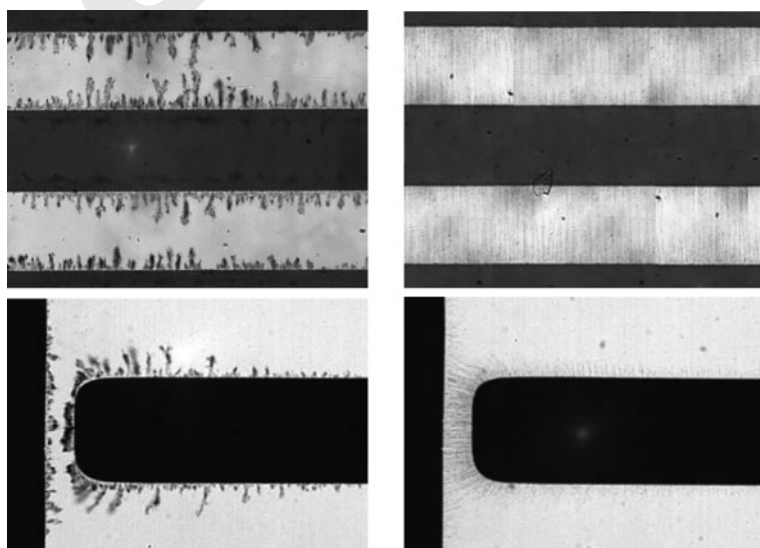


**Figure 1.** Nanotube self-assembly at 1 kHz (left column) and 1 MHz (right column) at SWNT concentration of 0.2 mg/mL under different frequency. Top two frames are for parallel electrodes 100  $\mu$ m in width and with a 100  $\mu$ m separation. Bottom frames are perpendicular electrodes of 160  $\mu$ m width and 50  $\mu$ m separation.

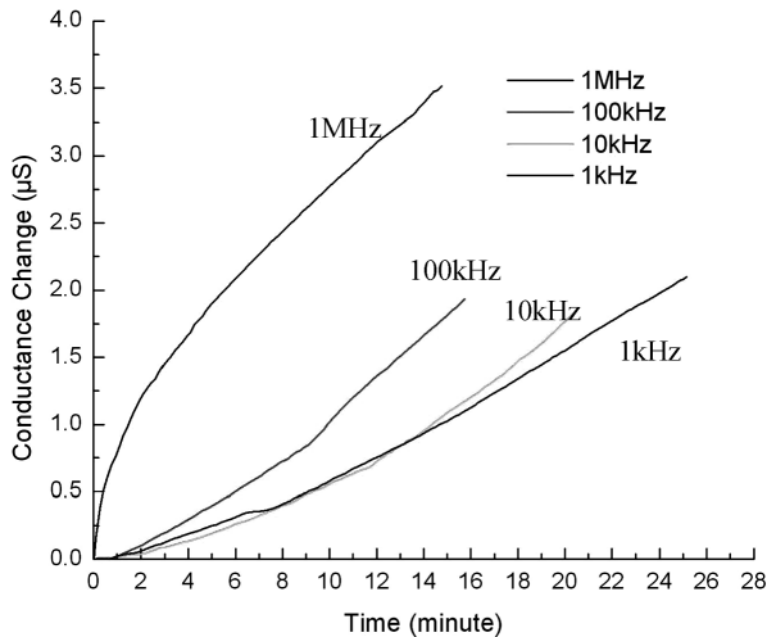


**Figure 2.** AC conductance measurements between the parallel electrodes of Fig. 1 for 0.2 mg/mL SWNT-COOH solution at different frequencies. AC conductance is defined as the inverse of the real part of the complex impedance.

the electrode. Hence, flow-breakup of wire bridges in Fig. 1a is unlikely. A more likely reason is that the field is confined to the electrode double layer at low frequencies. The electrode double layer and the bulk electrolyte can be considered as a double-layer capacitor with capacitance  $C_{DL}$  in series with an ohmic resistor with resistance  $R$ , both combining to produce a characteristic  $RC_{DL}$  time for the microelectrode array. When the frequency is below this inverse  $RC_{DL}$  time, the voltage drop is mainly across the thin double layer and the field is confined there. This localized field would explain the localized self-assembly at low frequencies. At frequencies higher than the inverse  $RC$  time, which is estimated to be about 10 kHz for the electrolyte used [11], the field penetrates across the bulk solution and hence self-assembly of the SWNT to bridge the gap is now feasible.

The critical frequency for bridging between the two electrodes can be measured with the aid of the circuit model shown in Fig. 3a that includes a parasitic circuit capacitance  $C$ . The impedance phase spectrum of this circuit, measuring the phase lag between the AC voltage and current, can be shown to be

$$\theta = \arctg\left(-\frac{(C + C_{DL})/\omega + \omega C C_{DL}^2 R^2}{C_{DL}^2 R}\right) \quad (2)$$

The low-frequency behavior is dominated by the double-layer capacitor and it shows the phase approach toward a pure capacitor phase of 90°. This phase relaxes to zero at intermediate frequencies when most of the AC current passes through the resistor with resistance  $R$ . At even

higher frequencies, it is the parasitic capacitance  $C$  that dominates and again a rise to 90° is expected. The phase angle hence exhibits a minimum at an optimum frequency, which is the reciprocal of  $RC_{DL}$  [6]. Measuring the impedance phase of the parallel microelectrodes, we find the phase to exhibit this expected dependence on frequency for a variety of liquids, including the SWNT solution. As seen in Fig. 3b, the optimal frequency for SWNT solution is around 1 kHz, which is lower than all other solutions except DI water. As the nanotube solvent is DI water, this reflects the increased bulk conductivity due to the presence of nanotubes. Its conductivity is comparable to that of a PBS buffer at  $1.5 \times 10^{-4}$  M with conductivity roughly five times higher than that of DI water. The inverse  $RC_{DL}$  time of 1 kHz is consistent with the self-assembly patterns of Fig. 1 and the conductance measurements of Fig. 2, which indicate that the transition to the bridging linear wire pattern occurs beyond 1 kHz. Beyond that frequency, the voltage across the electrode drops mainly in the bulk, instead of being confined to the double layers, thus offering a long-range DEP trap. The bulk field beyond this frequency also promotes SWNT polarization and self-assembly of linear aggregates that bridge the two electrodes along the electrical field lines.

For conductive SWNTs, we expect a very large absolute value of the dielectric constant. In fact, it has been suggested that the polarizability of conductive SWNTs is effectively infinite [20]. The direction of the AC dipole due to this polarization can be determined from the Clausius-Mossotti factor  $K = \text{Re}((\epsilon_p^* - \epsilon_m^*)/(\epsilon_p^* + 2\epsilon_m^*))$ . Due to the

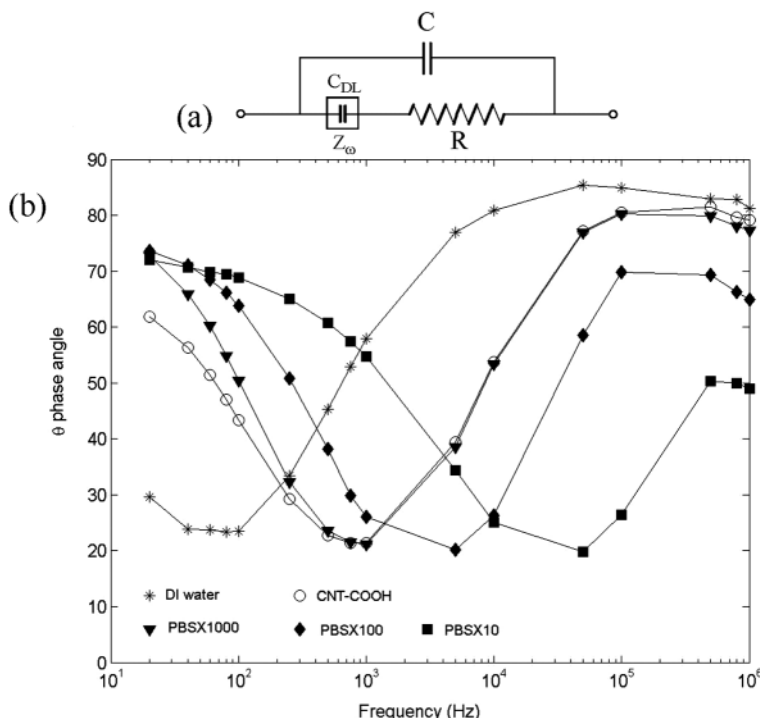


**Figure 3.** Equivalent circuit and phase angle measurements for the parallel electrode of Fig. 1 with the same SWNT concentrations. Phase angles of four other electrolytes are indicated. PBS solutions are diluted 1:10, 1:100, and 1:1000. Optimal frequency of the SWNT solution is slightly larger than that of DI water and is comparable to the 1:1000 PBS solution, indicating the SWNT has decreased the bulk resistance  $R$ . Optimal frequency of 1 kHz for the SWNT solutions represents the onset of linear wire bridges in the right column of Fig. 1 and the increase in measured conductance in Fig. 2.

large conductivity of SWNTs relative to the DI water medium, with the standard nanotube resistance of  $10^{-4} \Omega \times \text{cm}$  from literature [21], we find that SWNTs experience only positive DEP up to 10 MHz. This large positive-DEP mobility explains why SWNTs are trapped at the electrodes and self-assemble at 1 MHz. In comparison, *E. coli* experience positive DEP only near or below 10 kHz [6]. Beyond this frequency, cells experience negligible positive DEP and the trapping efficiency is low. Therefore, the strong positive-DEP force on the SWNT at 1 MHz can significantly enhance *E. coli* trapping if absorption of bacteria onto SWNTs or their bundles can be achieved in the bulk solution.

Evidence of this absorption is demonstrated with fluorescent particles in Fig. 4. Images of the trapped 500-nm and 1  $\mu\text{m}$  fluorescent particle images were recorded after 5 min for three different conditions at 1 MHz: fluorescent particles without SWNT, SWNT preassembled between the electrodes before the fluorescent particles were added, and a mixture of SWNT and fluorescent particles added before the field was activated. It is clear that the number of collected particles is quite similar for the case without SWNT and the case with pretemplated SWNT. Without SWNT wires, the electrode corners have the highest field and a small number of particles are trapped at that location. With the pretemplated wires bridging the electrodes, the high-field region is at the wire and trapping occurs directly onto the wire, although they still tend

to favor the ends of the wires closest to the electrode corners. As the particle DEP force is the same for both cases, similar trapping efficiency for the two indicate the corner field without SWNT and the field at the pre-templated wire are comparable in amplitude. In contrast, when SWNT is dispersed in the solution, nearly ten times as many particles are trapped. We attribute this enhanced efficiency to the higher positive-DEP mobility of the particles after absorption onto the SWNT.

To demonstrate that the particles have absorbed onto the SWNT in the bulk solution before the self-assembly occurs, we show images of the fluorescent particles as a function of time in Fig. 5. The fluorescent particles clearly appeared first near the electrodes and then invaded into the gap along the wire. This was exactly how the SWNT self-assembly pattern evolved in Fig. 1 and the self-assembly in Fig. 4 simply involved absorbed particles. The particles could not appear in the middle of the gap if the SWNTs self-assembled first without absorbing the particles.

A final verification of the bulk absorption mechanism is offered by changing the SWNT concentrations. In Fig. 6, the average fluorescent intensities (defined as the total units of the fluorescent intensity from a single particle in a  $50\mu\text{m} \times 50\mu\text{m}$  area between two electrodes) of the images are plotted as a function of time for pretemplated SWNT with two SWNT concentrations. It is clear from the fluorescence intensity that the lower SWNT curve is

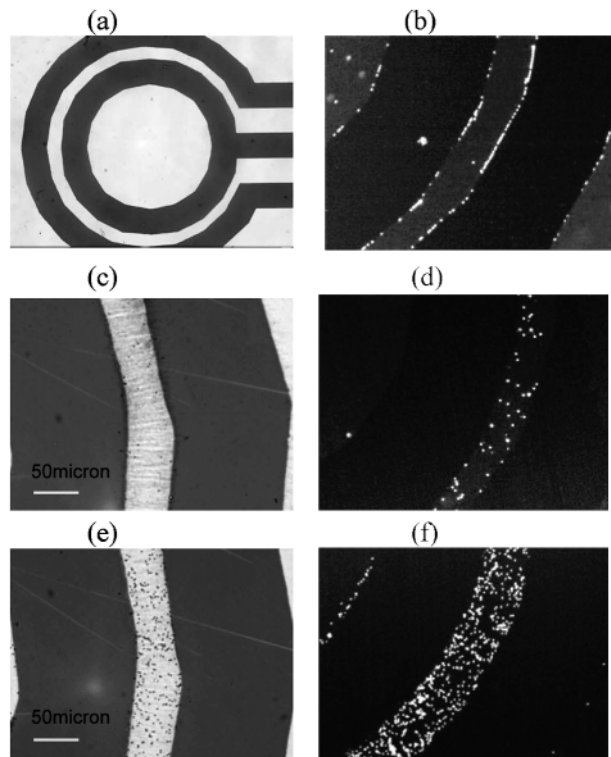


**Figure 4.** Fluorescent images taken at exactly 5 min after the electric field is activated for a circle electrode with a width of 160  $\mu\text{m}$ , a gap separation of 50  $\mu\text{m}$ . AC frequency is 1 MHz and 10 V. (a) Circle electrode configuration. (b) Forty microliters of 1  $\mu\text{m}$  or 500-nm particle suspension. SWNT suspension is not added. Particles collect at the high-field electrode corner. (c) Twenty microliters of SWNT suspension (0.2 mg/mL) is first placed on the electrode and the AC field is activated for 5 min to ensure that all the SWNT have formed linear wires between the electrodes. Image is taken 5 min later after the 20  $\mu\text{L}$  of particle suspension is added and mixed. (d) Fluorescent images of the particles. (e) SWNT and particle suspensions are premixed and then placed on the electrode before the field is activated. (f) Fluorescent image of the same assembly.

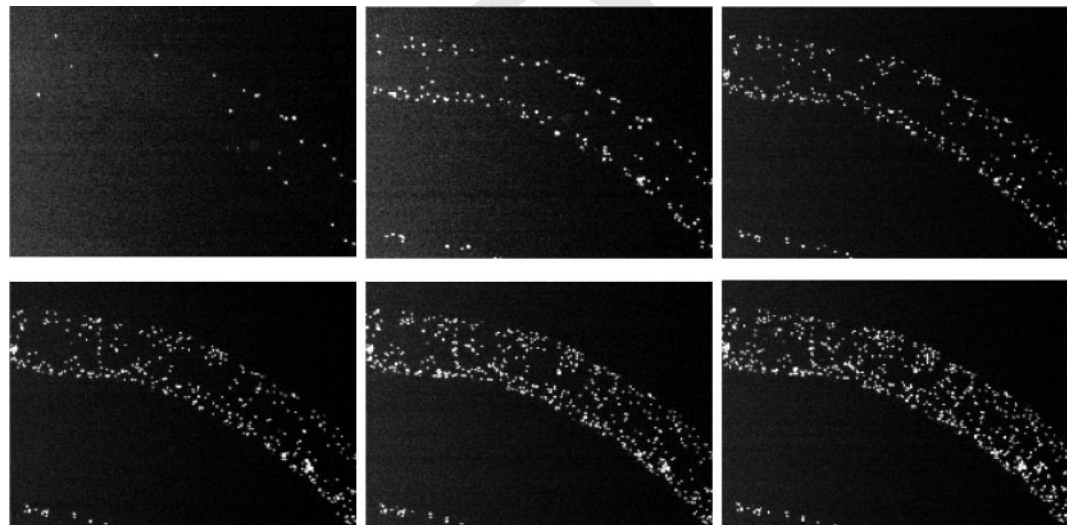


**Figure 5.** Successive fluorescent images of the particles with an interval of 30 s, starting from when the field is activated. Electrode configuration, voltages, and frequencies, and the suspension concentrations are identical to that of Fig. 4d.

shifted in time from the higher SWNT curve. This delay corresponds to the increased absorption time for a larger distance between particles and SWNT. More importantly, the intensity increases linearly in time with a rate that jumps discontinuously by a factor of 6–8 when the SWNT

concentration exceeds a critical value of 0.1 mg/mL. This is a direct indication that SWNT concentration affects the detection time and the detection threshold, which would only be true if the particle absorption occurs in the bulk. The critical suspension concentration of 0.1 mg/mL cor-

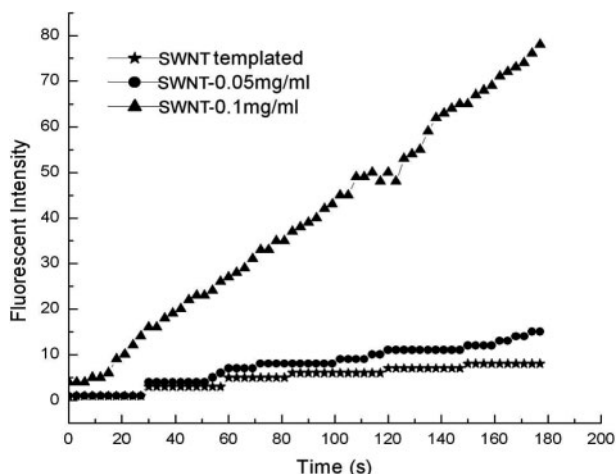


**Figure 6.** Fluorescence intensity curves as functions of time for three suspension mixtures corresponding to pre-templated SWNT and two SWNT concentrations of mixed particle/SWNT solution for particle collection. Fluorescent intensity unit is defined as the total number of fluorescent particles in a  $50 \mu\text{m} \times 50 \mu\text{m}$  area between the two electrodes.

responds to an SWNT separation of about  $1 \mu$ , which is also the tube length. Beyond this concentration, the field lines around each SWNT dipole overlapped,

thus saturating the entire solution with a nonuniform electric field that promotes DEP absorption of particles.

With the guidelines provided by the fluorescent particles, we test our technique with actual bacteria solution of *E. coli* at  $10^6$ ,  $10^5$ , and  $10^4$  CFU/mL. In Fig. 7a and b, trapping of  $10^5$  CFU/mL *E. coli* suspended in DI water and SWNT solution were compared. For bacteria concentration as low as  $10^4$  CFU/mL, an extremely small number of bacteria that exhibit weak positive DEP at 1 MHz were trapped at the edge of the electrodes after more than half an hour without SWNT. With the addition of SWNT, ten times more bacteria were trapped within 5 min. The trapped bacteria are entangled within the SWNT wires between the electrodes or sometimes next to the wires. The bacteria-SWNT aggregates visible in the images also suggest a side-to-side aggregation configuration, instead of the end-to-end self-assembly of SWNT. This lateral assembly pattern is consistent with the different induced dipole orientations and different mobility directions of the bacteria and the SWNT. The bacteria ( $10^6$  CFU/mL) were also stained with Rhodamine B (Sigma) as described in [22] and the fluorescent images in Fig. 7 again demonstrate that the addition of SWNT (d) enhances the trapping of bacteria at low concentrations compared to the case without SWNT (c).

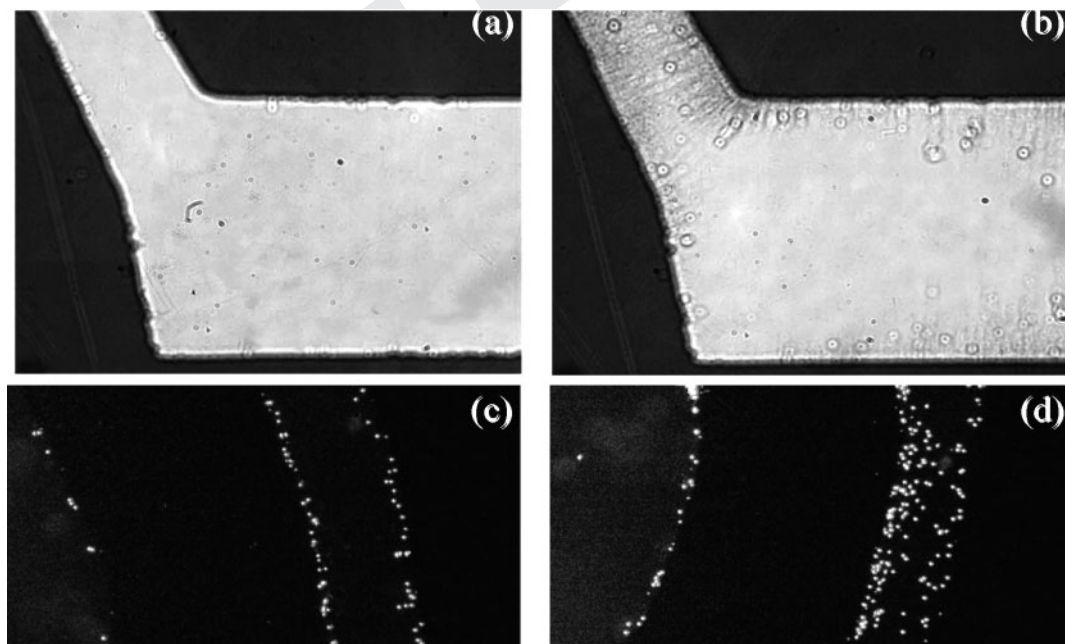


**Figure 7.** Bacteria trapping ( $10^5$  CFU/mL) without (a) and with SWNT ( $0.2 \text{ mg/mL}$ ) (b). Bacteria appear as transparent circles. Electrode configuration is the same as the fluorescent experiments of Fig. 5. Operating condition is 1 MHz with 10 V across the electrodes. Fluorescent bacteria trapping ( $10^6$  CFU/mL) under the same condition without (c) and with SWNT ( $0.2 \text{ mg/mL}$ ) (d) are imaged after staining with Rhodamine B.

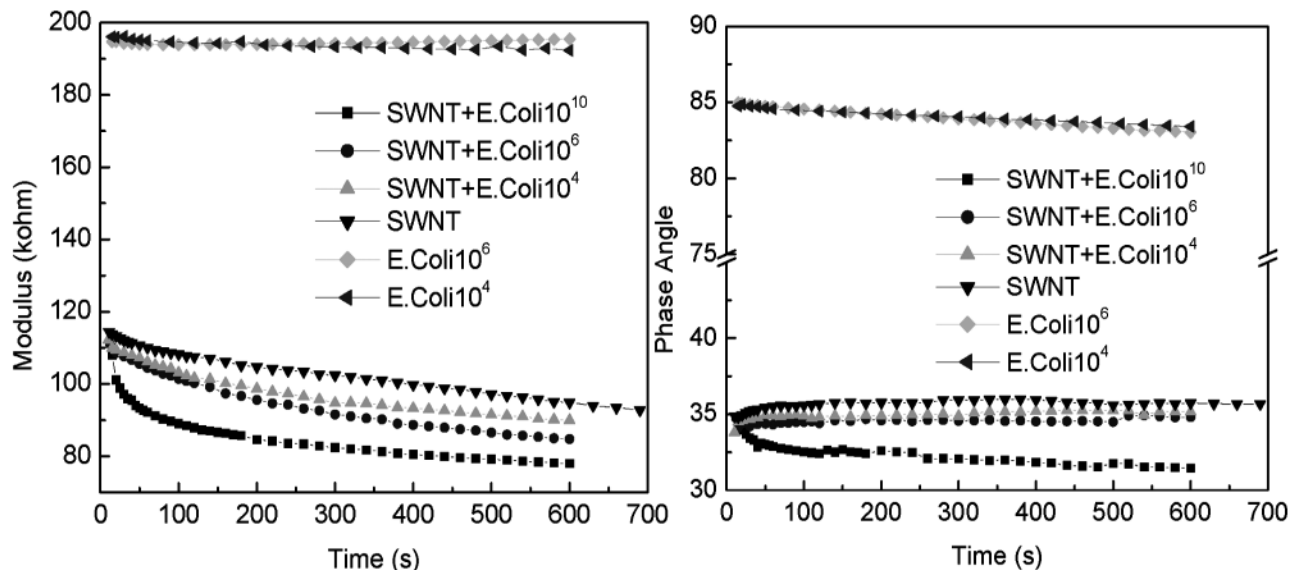


**Figure 8.** Impedance modulus and phase angle measured from the same trapping field at 1 MHz across the two electrodes in Fig. 7. Number of bacteria is varied for each run.

Voltage and current signals from the AC electrodes at 1 MHz were obtained during the self-assembly to record the variation in complex impedance as a function of time. These impedance data are shown in Fig. 8 for *E. coli* suspensions at  $10^{10}$ ,  $10^6$ , and  $10^4$  CFU/mL. The  $10^6$  and  $10^4$  CFU/mL bacteria solutions were compared for conditions with and without SWNT. In addition, SWNT self-assembly without bacteria was monitored as a reference. Without SWNT, the complex impedance of these  $10^6$  and  $10^4$  CFU/mL samples decreased slowly from the buffer value (without bacteria) over the entire 10-min measurement duration. The slow decline was due to the slow DEP capture of a small fraction of bacteria with positive DEP at the electrode corners. However, this decrease was not sensitive to bacteria count as only a few bacteria were attracted to the corners. As shown in Fig. 8, insufficient cells were trapped at the corner to discriminate between  $10^6$  and  $10^4$  CFU/mL in DI water without adding SWNT. It was evident that inserting SWNT significantly lowers the modulus and phase angle of the complex impedance, by as much as a factor of two, indicating that bridging had occurred between the electrodes. Moreover, the reduction was recorded within the first minute and the impedance signals for bacteria with SWNT reached their steady-state values after a short transient of 2 min. This short transient was also observed with the SWNT solution without bacteria. The difference in impedance signal for different bacteria counts was also evident in the first minute. These transient data then suggest that the SWNT bridges formed much faster than positive-DEP trapping of bacteria not absorbed onto SWNT. They also confirm that the bacteria

accompanied the SWNT during the bridge self-assembly, suggesting that the absorption had taken place in the bulk. With decreasing bacteria concentration, both modulus and phase increased until they approached the values without bacteria at about  $10^4$  CFU/mL.

The modulus signal showed stronger sensitivity to bacteria count but the fact that both modulus and phase were affected by the bacteria count at 1 MHz suggested that it was the bacterial capacitance that was affecting the complex impedance of the self-assembled bridge. As a result, DC conductance would not be able to provide the same detection sensitivity. Also, once assembled into the linear aggregate bridges, charge transfer across SWNT or bundles is now possible through the overlapping double layers and hence the capacitance of the linear aggregate should be much smaller than that of an isolated SWNT or bundle. The large internal capacitance of the pathogen can hence dominate the AC response despite the relative small fraction of bacteria within the bridge assembly. The AC impedance measurement indicated that the capacitance change produced by a bacteria count as low as  $10^4$  CFU/mL could be detected within a few minutes. In contrast, this small fraction of bacteria can never affect the DC conductance of the large bridge assembly. The change in AC signal due to bacteria capacitance can only occur if the bacteria are absorbed onto the SWNTs and are present within the bridges. In fact, Fig. 8 suggests that detection is possible in less than 2 min. Short of continuous imaging of the bacterial absorption and participation in the

bridge assembly, the impedance data offer good indirect evidence that detection sensitivity and time can be improved by SWNT addition.

#### 4 Concluding remarks

In conclusion, the high polarizability and positive DEP of SWNT in an AC field, whose crossover frequency is higher than the inverse *RC* time of the microelectrode array, are exploited to absorb particles in the bulk and to trap the absorbed particles, which would ordinarily exhibit weak positive DEP or even negative DEP, within the self-assembled SWNT wires between two electrodes. Preliminary results shown here indicate that this strategy of reducing the transport distance of small number of bioparticles to the sensor allows detection down to 10 000 particles *per* mL within 5 min with simple AC impedance spectroscopy by the same trapping electrodes and fields. With properly optimized electrode geometry and electrolyte composition and with more sensitive and functionalized bacteria detectors between the trapping electrodes, we expect to lower the detection threshold to 1000 particles *per* mL within the same detection time. Moreover, SWNT absorption onto immuno-assay beads and pathogens in a bulk AC field can also enhance the docking time of the beads and the pathogens. Functionalized SWNTs provide even more specificity. Hence, the role of SWNTs as absorbers and transporters of pathogens in a bulk AC field supplied by microfabricated electrodes can be profitably used in conjunction with other bacteria sensors in a variety of ways.

*This work is supported by NASA and NSF grants. We thank F. Liu from Dr. A. E. Ostafin's group and G. Kumar from Dr. P Kamat's group at the University of Notre Dame for valuable discussions.*

#### 5 References

- [1] Baughman, R. H., Zakhidov, A. A., de Heer, W. A., *Science* 2002, 297, 787–792.
- [2] Katz, E., Willner, I., *J. Chem. Phys.* 2004, 5, 1084–1104.
- [3] Qi, P., Vermesh, O., Grecu, M., Javey, A., Wang, Q., H. Dai., *Nano Lett.* 2003, 3, 347–351.
- [4] Chen, R. J., Choi, H. C., Bangsaruntip, S., Yenilmez, E. *et al.*, *J. Am. Chem. Soc.* 2004, 126, 1563–1568.
- [5] Patolsky, F., Zheng, G., Hayden, O., Lakadamyali, M. *et al.*, *Proc. Natl. Acad. Sci. USA* 2004, 101, 14017–14022.
- [6] Pohl, H. A., *Dielectrophoresis*, Cambridge University Press, Cambridge 1978.
- [7] Morgan, H., Green, N. G., *AC Electrokinetics: Colloids and Nanoparticles*, Research Studies Press, Baldock 2003.
- [8] Minerick, A., Zhou, R., Takhistov, P., Chang, H.-C., *Electrophoresis* 2003, 24, 3703–3717.
- [9] Lapizco-Encinas, B. H., Simmons, B. A., Cummings, E. B., Fintschenko, Y., *Electrophoresis* 2004, 25, 1695–1704.
- [10] Wong, P. K., Chen, C.-Y., Wang, T.-H., Ho., C.-M., *Anal. Chem.* 2004, 76, 6908–6914.
- [11] Wu, J., Ben, Y., Battigelli, D., Chang, H.-C., *Industr. Eng. Chem. Res.* 2005, 44, 2815–2825.
- [12] Hughes, M., Chen, G. Z., Shaffer, M. S. P., Fray, D. J., Windle, A. H., *Chem. Mater.* 2002, 14, 1610–1613.
- [13] Evoy, S., DiLello, N., Deshpande, V., Narayanan, A. *et al.*, *Microelectron. Eng.* 2004, 75, 31–42.
- [14] Cheng, C., Gonela, R., Haynie, D. T., *Nano Lett.* 2004, 5, 175–178.
- [15] Kamat, P. V., Thomas, K. G., Barazzouk, S., Girishkumar, G. *et al.*, *J. Am. Chem. Soc.* 2004, 126, 10757–10762.
- [16] Chen, X. Q., Saito, T., *Appl. Phys. Lett.* 2001, 78 3714–3716.
- [17] Zhang, Y., Chang, A., Cao, J., Wang, Q. *et al.*, *Appl. Phys. Lett.* 2001, 79, 3155–3157.
- [18] Englander, O., Christensen, D., Kim, J., Lin, L., Morris, S. J. S., *Nano Lett.* 2005, 5, 795–708.
- [19] Lastochkin, D., Zhou, R., Wang, P., Ben, Y., Chang, H.-C., *J. App. Phys.* 2004, 96, 1730–1733.
- [20] Krupke, R., Hennrich, F., Lohneysen, H. V., Kappes, M. M., *Science* 2003, 301, 344–347.
- [21] Data from Applied Nanotechnologies, Inc. website.
- [22] Abernethy, N. J., Chin, W., Lyons, H., Hay, J. B., *Cytometry* 1985, 6, 407–413.